

Properties of the Low Energy Nucleonic Component at Large Atmospheric Depths*

J. A. SIMPSON AND W. C. FAGOT

Institute for Nuclear Studies, University of Chicago, Chicago, Illinois

(Received February 13, 1953)

This is a report on the absorption properties of the cosmic radiation low energy nucleonic component measured by detectors of disintegration product neutrons as the nucleonic cascade develops deep within the atmosphere. The air absorption mean free path L of the star- or neutron-producing radiation was measured as a function of atmospheric depth x (in $\text{g}\cdot\text{cm}^{-2}$ atmosphere) at the geomagnetic latitudes $\lambda=0^\circ$, 41° , 52° . $L(x, \lambda)$ was obtained for carbon or free atmosphere and for a lead plus carbon pile geometry. As reported earlier, for small x the absorption mfp, L , is dependent upon λ (L is a function of the average energy of the primary nucleons which initiate the nucleonic chain or cascade). However, it is shown by the present measurements that, for $x > 600 \text{ g}\cdot\text{cm}^{-2}$, $L \rightarrow \sim 140 \text{ g}\cdot\text{cm}^{-2}$ independent of latitude λ .

The latitude dependence of neutron component intensity was measured at $x=680 \text{ g}\cdot\text{cm}^{-2}$ (11 200 ft) between $\lambda=0^\circ$ and 58°N . The latitude factor of intensity increase is 2.55. In view of the independence of $L(x)$ on λ at large atmospheric depths this latitude effect is nearly constant down to sea level ($x=1030$). It is shown that at large atmospheric depths neutron production is observed from primary protons with energies as low as ~ 1 Bev. The specific yield of neutrons at 11 200 ft has been computed taking into account protons, alpha-particles, and heavier primary nuclei.

These measurements resolve discrepancies reported in the literature between high altitude measurements and measurements between sea level and mountain altitudes for the low energy nucleonic component.

ALTHOUGH extensive measurements of the absorption of the star-producing radiations and fast neutrons from the nucleonic component have been obtained at both small and large atmospheric depths numerous discrepancies appear to exist among the measurements reported in the literature. For example, (a) extrapolations of the high altitude neutron or star intensity curves to sea level yield results inconsistent with the reported altitude dependence of stars in the lower atmosphere,^{1,2} and (b) the pressure coefficient for a neutron or low energy star detector as derived from intensity vs atmospheric pressure variations yields an equivalent absorption mean free path for the incident radiation which differs from intensity-altitude measurements higher in the atmosphere.³ In an attempt to resolve these difficulties and to extend the use of neutron detectors employed to measure nucleonic com-

ponent intensity-time variations at low latitudes, we have investigated some properties of the nucleonic component as a function of atmospheric depth. We have defined the low energy nucleonic component as the secondary component which is propagated by nucleons capable of producing nuclear disintegrations and which generates a cascade or chain of nucleons and nuclear disintegrations within the atmosphere. Each nuclear disintegration predominantly yields protons, neutrons, and alpha-particles. We shall measure nucleonic component intensity by detection of the disintegration product neutrons since the neutron intensity closely represents nucleonic component intensity and is easily measured.

Specifically, we shall report upon the absorption behavior of the nucleonic component in air as measured by fast disintegration neutron detectors as the nucleonic cascade or chain develops deep within the atmosphere of the earth. The study consists of measurements of the absorption mean free path L of the star-producing or neutron-producing radiation as a function of atmospheric depth x (in $\text{g}\cdot\text{cm}^{-2}$) and geomagnetic latitude λ . The measurements of $L(x, \lambda)$ were obtained for local production in carbon (equivalent to free atmosphere measurements⁴) and for local neutron production in a lead-carbon pile geometry. We also report on the latitude dependence over the range $\lambda=0^\circ-58^\circ$ for atmospheric depths between 11 000 ft and sea level. From these data we have computed the average neutron specific yield near sea level from incident primary particles of momentum-to-charge ratio P/Z .

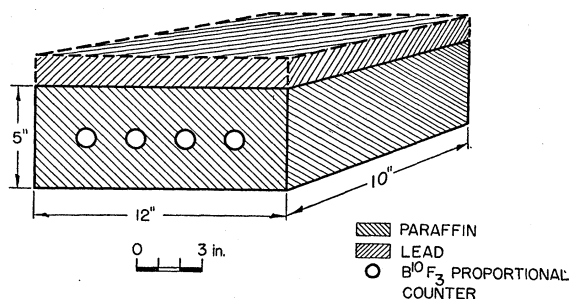


FIG. 1. Perspective view of detector. This is a pile geometry containing four B^{10}F_3 counters. Local production of neutrons from lead may be measured with the addition of a layer of lead as shown. This pile geometry was mounted in the nose section of an RF-80 aircraft. (See Fig. 2.)

I. DETECTORS AND INSTRUMENTATION

All the measurements, with the exception of one series of high altitude measurements at $\lambda=52^\circ$, were obtained with the geometry shown in Fig. 1. The geometry consisted of a paraffin block 5 in. \times 10 in. \times 12

* Assisted by the Office of Scientific Research, Air Research and Development Command, U. S. Air Force, Baltimore, Maryland.

¹ For example, M. Teucher, *Z. Naturforsch.* **7a**, 61 (1952).

² H. Yagoda, Proceedings of the Echo Lake Conference on Cosmic Rays (1949); J. G. Roederer, *Z. Naturforsch.* **7a**, 765 (1952).

³ V. Tongiorgi, *Phys. Rev.* **76**, 517 (1949); N. Adams and H. J. J. Braddick, *Z. Naturforsch.* **6a**, 592 (1951).

⁴ J. Simpson and R. B. Uretz, *Phys. Rev.* **90**, 44 (1953); J. Simpson, *Phys. Rev.* **83**, 1175 (1951).

in. in which four $B^{10}F_3$ proportional counters were distributed. Plates of lead 10 in. \times 12 in. were placed above the paraffin geometry as shown in Fig. 1 for measurements of local production in lead. For the measurements reported here the lead thickness was 59 g-cm^{-2} . Details on the behavior of pile geometries for measuring the local production of neutrons have been discussed in an earlier paper.⁴ We refer to local production within the paraffin block as production in carbon.

The detector system and associated electronic and recording apparatus were located in the nose section

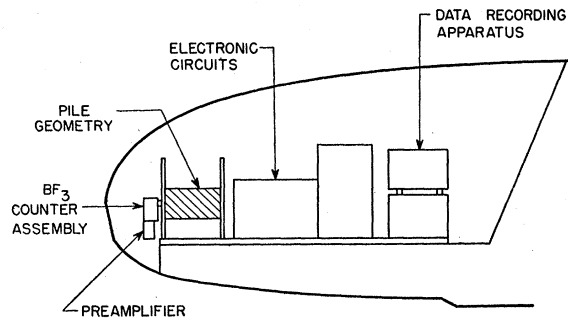


FIG. 2. Vertical view through mid-section of the RF-80 jet aircraft nose showing the location of the pile geometry (see Fig. 1) and related apparatus.

of a type RF-80 jet aircraft as shown in Fig. 2. Special aluminum ballast replaced the usual lead ballast required to balance the aircraft; there was no effect resulting from variable fuel loads.

The subminiature electronic circuits were designed specially for these measurements and will be described in detail elsewhere. By using a dual electronic and

TABLE I. The measurements of the air absorption mean free path $L(x)$ of the neutron-producing radiations at $\lambda=41^\circ\text{N}$.

Range of atmospheric depth, $x \text{ g-cm}^{-2}$	Flight No.	$L(x)$ carbon	$L(x)$ lead (59 g-cm^{-2})
240-380	257		162 ± 3
	262	175 ± 3	
	263		166 ± 3
	265	174 ± 3	
580-770	256		135 ± 3
	258		147 ± 3
	264	144 ± 4	

recording system the chance for component failure or loss of data was greatly reduced. All high potential circuits were maintained at sea level atmospheric pressure during all flights. Atmospheric pressure, accumulated counts, time and temperature were recorded at one minute intervals on film. An extra recorder was located in the cockpit so that the pilot could report preliminary results to a ground observer at specified intervals. The temperature in the nose section was controlled by a heated air stream from the aircraft heat-exchanger.

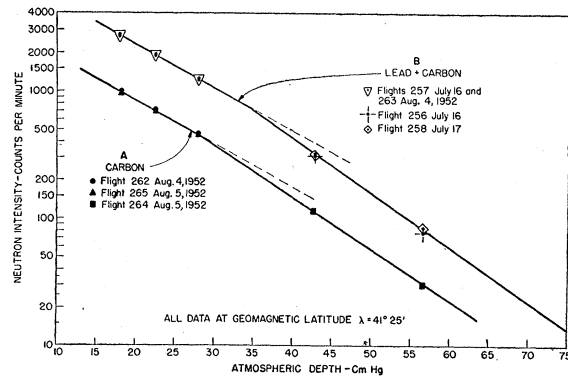


FIG. 3. The altitude dependence of the disintegration product neutron intensity at $\lambda=41^\circ 25'$ (Mobile, Alabama). From these data it is shown that the absorption mean free path L of the incident radiation is a function of atmospheric depth x . The experimental geometry for curve B is shown in Fig. 1 with lead thickness 59 g-cm^{-2} .

The pressure altimeter was modified to eliminate back lash or hysteresis effects and was calibrated to the N.A.C.A. standard atmosphere.

Before and after each flight the detector efficiency was checked with a Ra-Be neutron source. Since the counting rate of the detector at high altitude is the order of 1000-2500 events per minute, the neutron intensity at approximately 3-4 different altitudes may be obtained within the ~ 2 -hour fuel supply of the aircraft. Hence, the data for computing L from a single flight need not be corrected for intensity-time variations. For data assembled over extended periods of time the intensity corrections are obtained from our continuously operating pile detectors.⁵

II. DEGRADATION OF NUCLEON AVERAGE ENERGY WITH INCREASING ATMOSPHERIC DEPTH

We select first the intensity measurements at geomagnetic latitude $\lambda=41^\circ\text{N}$. The absorption of the neutron-producing radiation was computed on the assumption that over a small interval of atmospheric depth the omnidirectional intensity may be represented by $I=I_0e^{-x/L}$. The results are presented in Table I, and the data are plotted in Fig. 3 after correcting for the changes of primary intensity which occurred in July and August 1952. Curve A represents local production in carbon, air, and aircraft aluminum; curve B represents the addition of local production from lead 59 g-cm^{-2} thick. (See Fig. 1.)

At $\lambda=52^\circ\text{N}$ we report measurements of L in the range of $x=175$ to $x=750 \text{ g-cm}^{-2}$ atmosphere in Table II from a series of 32 flights. The average values of $L(x)$ for four ranges of x , with both the carbon and the lead geometries, are summarized in Table III.

For $\lambda=0^\circ$ values for L have been reported⁴ only for small values of x , i.e., $L=212 \text{ g-cm}^{-2}$ for $x \approx 200$ to $x \approx 500 \text{ g-cm}^{-2}$. Although measurements in aircraft

⁵ Simpson, Fonger, and Treiman, Phys. Rev. **90**, 934 (1953).

TABLE II. The measurements of the air absorption mean free path $L(x)$ of the neutron-producing radiations at $\lambda=52^\circ\text{N}$.

Range of atmospheric depth, x g-cm $^{-2}$	Flight No.	$L(x)$ carbon	$L(x)$ lead (59 g-cm $^{-2}$)
175-300	60*	166	
	61	177	
	62	164	
	63	165	
	64	171	
	66	162	
	68	172	
	69	166	
	70	168	
	71	169	
	74	173	
	75	162	
	76	168	
	77	170	
	78	168	
79	167		
247			165
248			155
249			163
251			158
230-530	138		148
	203	153	
	225	151	
	235		147
	266		150
	267		148
300-530	134	149	
	139	151	
	141	145	
530-750	144		136
	239		143
	240		139

* A cylindrical paraffin geometry was used for Flights 60-79.

were not obtained for large x at the equator, L has been determined⁵ from intensity measurements of carbon and carbon-plus-lead piles at two mountain altitudes in the range of $x=600-700$ g-cm $^{-2}$, with the results shown in Table IV.

We conclude from these experimental results that the absorption mean free path L for the neutron-producing radiation is a function of atmospheric depth x and that $L(x) \rightarrow 140$ g-cm $^{-2}$ near $x=700$ g-cm $^{-2}$. For example, in Fig. 3 at $\lambda=41^\circ$ $L(x)$ changes by 20 percent between $x \approx 300$ and $x=600$ for the free atmosphere and $L(x)$ changes by ~ 15 percent for local production in a lead-carbon pile. This latter result is a consequence of the reported anomalous measurements of L by using the local neutron production from elements of high atomic weight at small atmospheric depth.⁴

TABLE III. Summary of the data in Table II for $\lambda=52^\circ\text{N}$.

Range of atmospheric depth, x g-cm $^{-2}$	$L(x)$ carbon	$L(x)$ lead
175-300	168 ± 3	158 ± 2.3
230-530	152 ± 2	148 ± 2
300-530	148 ± 2	
530-750		141 ± 2

A crude plot of $L(x)$ vs x with λ as a parameter is given in Fig. 4. We conclude from these results that, in first approximation, $L(x)$ becomes independent of geomagnetic latitude at large atmospheric depths x .

Since it is known from cyclotron experiments with nucleons in the energy range of 50-450 Mev that L decreases with decreasing nucleon energy, it is clear that the change of L with x in the atmosphere is a consequence of the development of a nucleon cascade or chain. The nucleon average energy is degraded by nucleon collisions and nuclear disintegrations as the cascade develops deep within the atmosphere. These results are consistent with and an extension of the measurements of $L(\lambda)$ at small x , which show that as

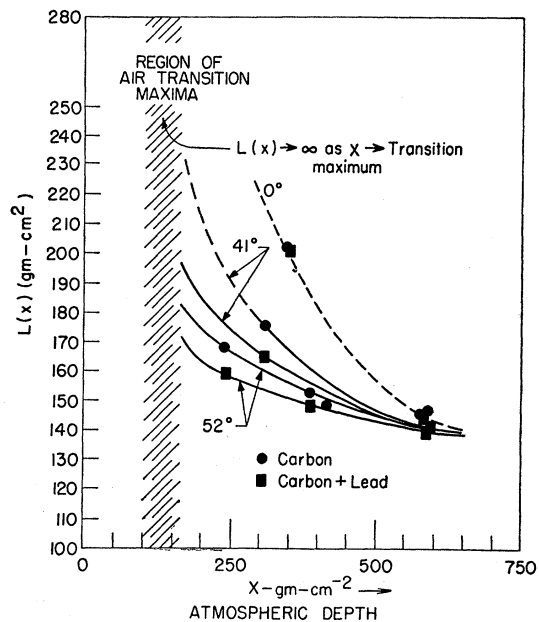


FIG. 4. The air absorption mean free path L as a function of atmospheric depth x at geomagnetic latitudes $\lambda=0^\circ$, 41°N and 52°N . The anomalous values of $L(x)$ at high altitude measured by determining local production rates in lead are shown. This phenomenon was discussed in reference 4.

the average primary particle nucleon energy is decreased, L decreases. We believe that any detailed theory providing for a description of the nucleonic cascade must account for this behavior of $L(x)$.

III. INTERPRETATION OF RELATED MEASUREMENTS

We may now explain the apparent anomaly between the atmospheric pressure coefficient ("barometric" coefficient) and the absorption mean free path measurements for neutron production by the nucleonic component. Several observers have reported measurements of the pressure coefficient for neutron production. All the measurements were at high latitudes and at altitudes below 14 000 ft pressure altitude. The values obtained

are in the range -0.92 to -1.1 percent/mm Hg, which leads to an absorption mean free path of $L \approx 140 \text{ g-cm}^{-2}$.³ This L is now in agreement with the free air absorption measurements in the *lower atmosphere*. Further, we conclude that within experimental errors the pressure coefficient for local neutron production in the lower atmosphere is *not* a function of λ . This result is of interest where the local neutron production is used as a monitor of intensity variations at low latitudes, but where the small tropical pressure variations have made it difficult to obtain an accurate pressure coefficient for $\lambda = 0^\circ$.⁵

Photographic plate measurements in the lower atmosphere yield $L = 130\text{--}145 \text{ g-cm}^{-2}$ for the star-producing radiation. Our measurements also explain the observations of Yagoda and Roederer² at low altitudes, in which the altitude dependence of star production was approximately independent of λ .

The recent low altitude measurements of fast neutron production at $\lambda = 20^\circ$ by Curtiss and Gill⁶ are now clearly related to the high altitude neutron production at this latitude.

IV. LATITUDE DEPENDENCE OF NEUTRON PRODUCTION IN THE LOWER ATMOSPHERE

For $x > 600 \text{ g-cm}^{-2}$ we have shown that $L(x)$ is independent of λ in first approximation. We therefore report I vs λ measurements for $x > 600$, since this latitude effect will be essentially constant with x in the lower atmosphere. The results are given in Fig. 5 for $x = 681 \text{ g-cm}^{-2}$, where measurements above 40° were obtained with the carbon plus 59 g-cm^{-2} thick lead pile in the jet aircraft. All data are corrected for variations with time and normalized to the average intensity observed October 6, 1952. The points at 0° , 29° , 42° , and 48° are obtained from the ratios of neutron production in "standard" piles⁵ employed for observing intensity-time variations near 11 000 ft; these points are normalized to the pressure $x = 681 \text{ g-cm}^{-2}$. These data are then fitted to the aircraft results at $\lambda = 48^\circ \text{N}$. Since $L(x)$ is independent of λ for $x > 600$, we conclude that at $x = 681$ the neutron production increases by the factor 2.55 from the geomagnetic equator to $> 58^\circ$ and the increase is only slightly less at *sea level* ($x = 1030$). The shape of the latitude curve, Fig. 5, for intermediate latitudes is determined by the *longitude* dependence of the neutron intensity. We therefore note that the intermediate point at 29° was determined at 99° west longitude. The only reported latitude measurement of stars in photographic emulsions near this altitude is in agreement with this neutron latitude effect.⁷

Although the exact shape of the curve in Fig. 5 has not been determined above 52° , we observe that $dI/d\lambda \rightarrow 0$ as $\lambda \rightarrow 56^\circ \text{N}$. From this fact we estimate the *minimum* momentum-to-charge ratio of a primary

TABLE IV. The measurements of the air absorption mean free path $L(x)$ of the neutron-producing radiations at $\lambda = 0^\circ \text{N}$.

Range of atmospheric depth, $x \text{ g-cm}^{-2}$	$L(x)$ carbon or lead g-cm^{-2}
200-500	212 ± 4
600-700	145 ± 9

particle producing secondary particles which contributes to the total neutron production at sea level. For a centered dipole geomagnetic field this value is $\sim 1 \text{ Bev/c}$ for vertically incident primary protons. This observed low momentum cutoff is either: (1) due to atmospheric absorption of the primary particles of lowest momenta and their secondaries, or (2) due to a cutoff in the primary particle spectrum. Recent evidence discussed in reference 5 favors a primary spectrum cutoff.

V. SPECIFIC YIELD OF NEUTRONS AT LOW ALTITUDES

The specific yield for neutrons has been defined in reference 5 as a function $S(P/Z, x)$ which gives the observed time-averaged neutron counting rate at atmospheric depth x arising from a unity flux of vertically incident primary particles of momentum-to-charge ratio P/Z . We may rewrite Eq. (2) in reference 5 in terms of particle kinetic energy per nucleon as follows:

$$I_v(\lambda, x, t) = \sum_Z \int_{EZ(\lambda, t)}^{\infty} S_Z(E, x) j_Z(E, t) dE \quad (1)$$

at time t , where I_v is the neutron intensity at λ, x, t arising from the vertically incident primary particles. Since for $x > 600 \text{ g-cm}^{-2}$ $L(x)$ is independent of lati-

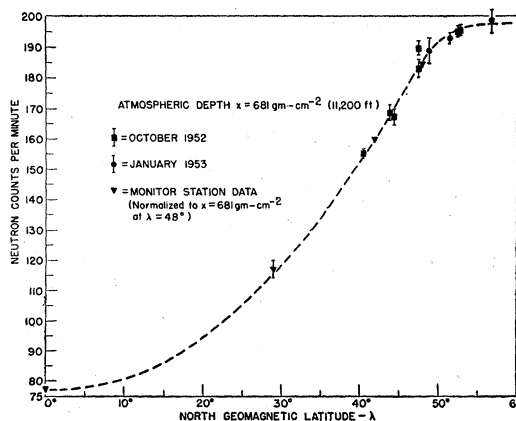


Fig. 5. Disintegration product neutron intensity (low energy nucleonic component intensity) as a function of geomagnetic latitude λ . This is the approximate curve for all greater atmospheric depths including sea level. The monitor station data are obtained from continuous recording piles described in reference 5. The shape of the curve near $20\text{--}35^\circ \text{N}$ is determined by the longitude effect.

⁶ L. F. Curtiss and P. S. Gill, Phys. Rev. **85**, 309 (1952).

⁷ S. Lattimore, Phil. Mag. **41**, 961 (1950).

tude λ , we have from Eq. 3, reference 5, $I_v \propto I$, where I is the counting rate of the omnidirectional detector.

If we separate $S_Z(E, x)$ to form the product of two functions, one dependent on Z , the other dependent on E and x , then

$$S_Z(E, x) = k_Z S(E, x), \quad (2)$$

where $k_Z \approx A$, the atomic weight of the primary particle.⁵ Accordingly,

$$I_v = (\lambda, x, t) = \sum_Z k_Z \int_{E_Z(\lambda, t)}^{\infty} S(E, x) j_Z(E, t) dE. \quad (3)$$

Fonger⁸ has fitted the function $S(E, x)$ to the experimental data shown in Fig. 5 for the omnidirectional detector at 0° and above 40° for $x = 680$ g-cm⁻². The primary differential spectra are obtained from Kaplon

⁸ W. H. Fonger, thesis, University of Chicago, 1953 (unpublished).

*et al.*⁹ The results are as follows:

$$S(E, 680) = \begin{cases} 0 & \text{for } E < E_0, \\ 9.64 \ln[(1+E)/(1+E_0)] & \text{for } E > E_0, \end{cases} \quad (4)$$

where E_0 is 0.83 Bev. The computed detector counting rate was normalized to unity at $\lambda = 0^\circ$.

This function will generate an intensity *vs* latitude curve which falls below the experimental curve in Fig. 5 at intermediate latitudes since we do not take account of the longitude effect.

We are indebted to the many pilots, ground crews, and the staff at the Flight Test Division, Wright Air Development Center, U.S.A.F. for their generous cooperation and expert assistance in this work. We also wish to express our thanks to L. Wilcox, K. Benford, W. H. Fonger, R. Baron, and Dr. S. B. Treiman for assistance.

⁹ Kaplon, Peters, Reynolds, and Ritson, Phys. Rev. **85**, 295 (1952).

A Note on Meson-Nucleon Scattering

ROBERT KARPLUS, MARGARET KIVELSON, AND PAUL C. MARTIN*

Harvard University, Cambridge, Massachusetts

(Received March 3, 1953)

A relativistic meson-nucleon two-body equation applicable to the elastic nonexchange scattering of negative pions by protons is solved using the lowest order interaction kernel. The scattering matrix which this equation yields is shown to be unitary. The total cross section calculated from this scattering matrix is finite at threshold and relatively independent of the coupling constant. A plot of the cross section as a function of energy is included.

THE relativistic two-body equation^{1,2} has proved useful³ in discussing the behavior of two-nucleon systems. With this equation one may attempt to get approximate solutions by using terms from the expansion of the interaction operator in powers of the coupling constant, but not assuming such an expansion for the meson-nucleon Green's function itself.⁴ The three-dimensional approximation to the resulting equation is equivalent to the configuration space or generalized Tamm-Dancoff method.³ The latter has the disadvantage that self-energy terms cannot be readily recognized and removed. In the case of negative pion proton elastic nonexchange scattering that part of the lowest order kernel which leads to divergences is so simple that with this term alone we may solve the four-dimensional integral equation directly. Renor-

malization may then be carried out in the usual manner. The scattering matrix for the process calculated from this Green's function can be shown to be unitary. For meson energies above a few hundred Mev the calculated cross section is almost independent of the coupling constant; even at low energies the *s* wave scattering is insensitive to the choice of coupling constant in the usual range of values.

We begin with the relativistic meson-nucleon two-body equation. Using the notation of the previous papers,^{2,4,5} this may be written

$$[(\gamma p + M)(k^2 + \mu^2 + \Pi) - I_{MN}]G_{MN} = 1. \quad (1)$$

We retain only that part of the interaction operator which gives rise to the above-mentioned divergence difficulty,

$$(x\xi | I_{MN} | y\eta) = -ig^2\gamma_5\tau^k G_+^{(0)}(x-x')\gamma_5\tau^l \times \delta(x-\xi)\delta(y-\eta). \quad (2)$$

⁵ S. F. Edwards, Phys. Rev. **90**, 284 (1953).

* National Science Foundation Predoctoral Fellow.

¹ H. A. Bethe and E. E. Salpeter, Phys. Rev. **84**, 1232 (1951).

² J. Schwinger, Proc. Natl. Acad. Sci. U. S. **37**, 452, 455 (1951).

³ M. Levy, Phys. Rev. **88**, 441 (1952); A. Klein, Phys. Rev. **90**, 1101 (1953).

⁴ S. Deser and P. Martin, preceding paper [Phys. Rev. **90**, 1075 (1953)].